The Life Cycle Stages of *Pneumocystis murina* Have Opposing Effects on the Immune Response to This Opportunistic Fungal Pathogen

Heather M. Evans,[a] Grady L. Bryant III,[a] Beth A. Garvy[a,b]

Department of Microbiology, Immunology, and Molecular Genetics[a] and Division of Infectious Diseases, Department of Internal Medicine,[b] University of Kentucky College of Medicine, Lexington, Kentucky, USA

The cell wall β-glucans of *Pneumocystis* cysts have been shown to stimulate immune responses in lung epithelial cells, dendritic cells, and alveolar macrophages. Little is known about how the trophic life forms, which do not have a fungal cell wall, interact with these innate immune cells. Here we report differences in the responses of both neonatal and adult mice to the trophic and cystic life cycle stages of *Pneumocystis murina*. The adult and neonatal immune responses to infection with *Pneumocystis murina* trophic forms were less robust than the responses to infection with a physiologically normal mixture of cysts and trophic forms. Cysts promoted the recruitment of nonresident innate immune cells and T and B cells into the lungs. Cysts, but not trophic forms, stimulated increased concentrations of the cytokine gamma interferon (IFN-γ) in the alveolar spaces and an increase in the percentage of CD4$^+$ T cells that produce IFN-γ. *In vitro*, bone marrow-derived dendritic cells (BMDCs) stimulated with cysts produced the proinflammatory cytokines interleukin 1β (IL-1β) and IL-6. In contrast, trophic forms suppressed antigen presentation to CD4$^+$ T cells, as well as the β-glucan-, lipoteichoic acid (LTA)-, and lipopolysaccharide (LPS)-induced production of interleukin 1β (IL-1β), IL-6, and tumor necrosis factor alpha (TNF-α) by BMDCs. The negative effects of trophic forms were not due to ligation of mannose receptor. Our results indicate that optimal innate and adaptive immune responses to *Pneumocystis* species are dependent on stimulation with the cyst life cycle stage. Conversely, trophic forms suppress β-glucan-induced proinflammatory responses *in vitro*, suggesting that the trophic forms dampen cyst-induced inflammation *in vivo*.

Pneumocystis species are opportunistic fungal pathogens that cause severe pneumonia in immunocompromised hosts, including AIDS patients. Clearance of *Pneumocystis* organisms is dependent on effective CD4$^+$ T and B cell and macrophage responses [1–4]. Failure to clear *Pneumocystis* organisms leads to severe alveolar damage due to the exaggerated inflammatory immune response [5]. In spite of a reduced incidence of *Pneumocystis* pneumonia (PcP) in HIV-infected individuals due to improved antiviral therapies, the mortality rate for patients with PcP has not improved with the implementation of highly active antiretroviral therapy (HAART) [6]. Additional studies are required to inform novel approaches to reduce morbidity and mortality due to *Pneumocystis* pneumonia.

Outbreaks of PcP were first described in malnourished or premature infants in orphanages following the Second World War [7]. Evidence suggests that immunocompetent individuals of all ages are capable of mounting protective immune responses to *Pneumocystis jirovecii* that prevent progression to pneumonia. Most children encounter this opportunistic fungus at a young age, as indicated by the presence of specific antibodies in the sera of 85% of individuals by the age of 3 years [8]. Previous work from our lab has shown that the neonatal mouse immune response to *Pneumocystis* is delayed, due in part to an anti-inflammatory lung environment [9–12]. The neonatal lung environment is characterized by anti-inflammatory mediators, including transforming growth factor β1 (TGF-β1) and interleukin 10 (IL-10), and immature immune cells [9–12]. Neonatal alveolar macrophages and T cells adoptively transferred to an adult lung environment are competent at resolving *Pneumocystis murina* pneumonia in mice [9, 12]. In addition, neonatal alveolar macrophages are deficient in NF-κB translocation following stimulation with *Pneumocystis* organisms [9]. Neonatal alveolar CD11c$^+$ cells demonstrate delayed trafficking to the draining lymph nodes [11]. Together, these

data indicate that both the neonatal lung environment and intrinsic immune cell deficits contribute to the delayed clearance of *P. murina* in neonatal mice.

Pneumocystis species have a biphasic life cycle. Trophic forms are proposed to represent the asexual stage of the life cycle, whereas cysts are the ascus-like sexual stage [13]. Trophic forms are single-nucleated organisms that are typically found in clusters surrounded by a biofilm-like substance consisting of a conglomeration of DNA, β-glucan, and other sugars [14]. Cysts are ascus-like structures that consist of multiple nuclei surrounded by a fungal cell wall. β-1,3-Glucan and β-1,6-glucan serve as the structural components of the cyst wall [15, 16]. Trophic forms do not express β-glucan [15]. Both stages express surface glycoproteins and mannoproteins, which may serve as pathogen-associated molecular patterns (PAMPs) that could interact with receptors on phagocytic cells [17–19]. Neither life form expresses chitin or α-glucans [20].

Dendritic cells are the principal antigen-presenting cells in the lung. However, their role in initiating the adaptive response to

Pneumocystis organisms has been understudied. Previous work has demonstrated that dendritic cells respond to β-glucans derived from the *Pneumocystis* cell wall (21). Dendritic cells activated by *Pneumocystis* cell wall-derived β-glucans increase costimulatory molecule expression and drive T cell polarization toward a T_h1-type response (21). The mechanism for dendritic cell recognition of *Pneumocystis* trophic forms, which do not express β-glucans, is unknown.

Improved understanding of innate immune interactions with the cystic and trophic life cycle stages has the potential to inform future treatment of *Pneumocystis* pneumonia. Recently, it was reported that treatment of mice with the β-1,3-D-glucan synthase inhibitor anidulafungin resulted in depletion of *P. murina* cysts (22). The mice were able to control the remaining trophic burden in the absence of an excessive inflammatory response; however, the details of how trophic forms are recognized and cleared are not known.

In this study, we demonstrate that both the adult and the neonatal immune responses to infection with *P. murina* trophic forms alone were less robust than the responses to infection with a physiologically normal mixture of cysts and trophic forms. Infection with trophic forms alone resulted in less recruitment of activated $CD4^+$ and $CD8^+$ T cells into the lungs of both neonatal and adult mice than infection with a normal mixture of trophic forms and cysts. Infection with a mixture of *P. murina* organisms drove the recruitment of nonresident innate immune cells into the lung parenchyma and alveolar spaces. *In vitro*, trophic forms suppressed the production of the proinflammatory cytokines IL-1β, IL-6, and tumor necrosis factor alpha (TNF-α) by bone marrow-derived dendritic cells (BMDCs) stimulated with β-glucan, lipoteichoic acid (LTA), or lipopolysaccharides (LPS). In addition, trophic-form-stimulated BMDCs failed to stimulate production of the T_h1-type cytokine gamma interferon (IFN-γ) by $CD4^+$ T cells. We report for the first time that the trophic forms of *P. murina* suppress β-glucan-induced proinflammatory responses.

MATERIALS AND METHODS

Mice. Six-week-old BALB/cJ, dectin-1 knockout (dectin-1 KO; B6.129S6-Clec7a^tm1Gdb^/J) and mannose receptor knockout (MR$^{-/-}$; B6.129P2-Mrc1^tm1Mnz^/J) mice were purchased from The Jackson Laboratory (Bar Harbor, ME) and were bred in our animal facilities. Male and female pups were used in the neonatal experiments. Six-week-old female BALB/cJ mice were purchased from The Jackson Laboratory and were infected at the age of 8 weeks either for the adult experiments or to generate $CD4^+$ T cells for the *in vitro* experiments. Uninfected adult female BALB/cJ, dectin-1 KO, MR$^{-/-}$, and B6.129P2 mice from The Jackson Laboratory were used to generate BMDCs for the *in vitro* experiments. Mice were maintained at the University of Kentucky Department of Laboratory Animal Resources (DLAR) under specific-pathogen-free conditions. C.129S6(B6)-Rag2^tm1Fwa^ N12 (Rag2$^{-/-}$) mice, originally from Taconic (Germantown, NY), were used to maintain a source of *P. murina* and were bred at the DLAR in sterile microisolator cages with sterilized food and water. The University of Kentucky Institutional Animal Care and Use Committee approved all protocols regarding animal use.

***P. murina* isolation and infection.** Lungs were excised from *P. murina*-infected Rag2$^{-/-}$ mice and were pushed through stainless steel mesh in Hanks' balanced salt solution (HBSS) containing 0.5% glutathione at pH 7.3. Cell debris was broken up by aspirating through 20- and 26-gauge needles and was then removed by centrifugation at $100 \times g$ for 3 min. Trophic forms were isolated by removing the supernatant following centrifugation at $400 \times g$ for 7 min. This preparation results in >99% pure trophic forms (see Fig. S1 in the supplemental material). The pellet from the $400 \times g$ spin contained a mixed population of cysts and trophic forms, at a typical ratio of 10:1 (trophic forms to cysts). Erythrocytes in the pellet were lysed with water, and organisms were suspended in an equal volume of $2\times$ phosphate-buffered saline (PBS). Organisms were incubated with 200 U DNase (Sigma-Aldrich, St. Louis MO) at 37°C for 30 min. Clumps were broken up by aspirating through a 26-gauge needle. The remaining cell debris was removed by centrifugation at $100 \times g$ for 3 min, followed by passage over a 70-μm filter. Aliquots of mixed *P. murina* organisms or purified trophic forms were diluted, and 100-μl aliquots were spun onto a 28.3-mm^2 area of glass slides. Slides were fixed in methanol and were stained with Diff-Quik (Siemens Healthcare Diagnostics, Inc., Deerfield, IL). Organism numbers were determined microscopically using the $100\times$ oil immersion objective of a Nikon microscope.

Mice were anesthetized lightly with isoflurane anesthesia to suppress the diver's reflex. Neonatal mice (24 to 72 h old) were inoculated intranasally (i.n.) with 10^6 trophic or mixed *P. murina* organisms in 10 μl HBSS containing 10 U/ml penicillin, 10 μg/ml streptomycin, and 1 μg/ml gentamicin. Adult mice (6 to 8 weeks old) were inoculated intratracheally (i.t.) with 10^7 trophic or mixed *P. murina* organisms in 100 μl HBSS containing antibiotics. The adult mice were placed on an upright support rack, and the inoculations were performed using a blunted intratracheal needle designed with a curve to accommodate the trachea.

Isolation of cells from alveolar spaces, lungs, and lymph nodes. Mice were exsanguinated under deep isoflurane anesthesia, and lungs were lavaged with 5 washes of HBSS containing 3 mM EDTA. Bronchial alveolar lavage fluid (BALF) was centrifuged to obtain cells, and the cell-free supernatant from the first wash was frozen for subsequent cytokine assays. Right lung lobes were excised, minced, and digested in RPMI medium containing 3% heat-inactivated fetal calf serum, 1 mg/ml collagenase A (Sigma-Aldrich, St. Louis MO), and 50 U/ml DNase for 1 h at 37°C. Digested lungs were pushed through 70-μm nylon mesh screens to obtain single-cell suspensions, and aliquots were taken for enumeration of *P. murina*. Tracheobronchial lymph nodes (TBLN) were also excised and were pushed through 70-μm nylon mesh screens in HBSS. Erythrocytes were removed using hypotonic ammonium-chloride-potassium (ACK) lysing buffer. Cells were washed and were counted by hemocytometer.

Flow cytometric analysis. BALF, lung digest, and TBLN cells were washed with PBS containing 0.1% bovine serum albumin and 0.02% NaN$_3$ and were stained with appropriate concentrations of fluorochrome-conjugated antibodies specific for murine lymphocytes (anti-CD4 clone GK1.5, anti-CD8a clone 53-6.7, anti-CD19 clone 1D3, anti-CD44 clone IM7, and anti-CD62L clone MEL-14) or innate immune cells (anti-CD11c clone N418, anti-CD11b clone M1/70). Antibodies were purchased from BD Biosciences (San Jose, CA) or eBioscience (San Diego, CA). Expression of these molecules on the surfaces of the cells was determined by multiparameter flow cytometry using an LSR II flow cytometer (BD Biosciences). A total of 50,000 events were routinely acquired and were analyzed using FlowJo software (TreeStar, USA).

Enumeration of *Pneumocystis* organisms in the lungs of mice. Aliquots of lung homogenates were spun onto glass slides and were stained as described above. The number of *P. murina* trophic forms or cysts in 50 microscopic oil immersion fields was used to calculate fungal burden. Lung burden is expressed as the number of *P. murina* organisms per right lung lobe, and the limits of detection were $\log_{10}$ 3.12 nuclei per neonatal right lung lobe and $\log_{10}$ 3.42 nuclei per adult right lung lobe.

Generation of BMDCs and $CD4^+$ T cells for *in vitro* assays. BMDCs were generated from uninfected BALB/cJ, B6.129P2, dectin-1 KO, and MR$^{-/-}$ adult female mice. BMDCSs were produced by flushing cells from the bone marrow of the tibias and femurs of female adult mice with PBS plus 5% heat-inactivated fetal bovine serum (FBS; Atlas Biologicals, Fort Collins, CO). Erythrocytes were removed using ACK lysing buffer (23). Cells were washed and were resuspended in a culture medium containing RPMI medium with 10% heat-inactivated FBS, 0.5 mM 2-mercaptoethanol, 1% MEM nonessential amino acid solution (ATCC, Manassas, VA), 100 U/ml penicillin, 100 μg/ml streptomycin, and 50 μg/ml gentamicin

(Thermo Fisher Scientific, Waltham, MA). Cells were plated in 100-mm petri dishes at a density of 4×10^6 in 10 ml culture medium with 20 ng/ml recombinant murine granulocyte-macrophage colony-stimulating factor (GM-CSF; Peprotech, Rocky Hill, NJ). Plates were cultured at 37°C under 5.0% CO_2. An additional 10 ml of culture medium with 20 ng/ml recombinant murine GM-CSF was added to cells after 24 h of growth. Every 48 h thereafter, nonadherent cells were removed and were replaced with 10 ml of fresh medium containing recombinant murine GM-CSF. Cells were cultured for 9 to 12 days. BMDCs were collected by vigorously washing plates with medium to remove loosely adherent cells. BMDCs were washed, resuspended, and split for phenotyping or a cytokine assay. More than 80% of recovered cells were CD11c$^+$. CD4$^+$ T cells were generated by infecting adult BALB/cJ mice with 10^7 mixed *P. murina* organisms as described above. TBLN were excised 10 to 14 days postinfection and were pushed through 70-μm nylon mesh screens in HBSS. Erythrocytes were removed using ACK lysing buffer. Cells were washed and counted. CD4 (L3T4) microbeads (Miltenyi Biotec, San Diego, CA) were used for positive selection of CD4$^+$ cells. More than 90% of recovered cells were CD4$^+$ T cells.

***In vitro* cytokine production assays.** A total of 10^4 BMDCs and/or 5×10^4 CD4$^+$ T cells in 96-well plates were stimulated with 10 μg/ml curdlan (β-1,3-glucan from *Alcaligenes faecalis*; Sigma-Aldrich), 20 μg/ml zymosan (*Saccharomyces cerevisiae* cell wall; Sigma-Aldrich), 20 μg/ml depleted zymosan (InvivoGen, San Diego, CA), 10 μg/ml lipoteichoic acid (LTA) (from *Bacillus subtilis*; Sigma-Aldrich), 100 ng/ml lipopolysaccharides (LPS) (from *Escherichia coli* 0111:B4; purified by gel filtration to remove lipoproteins; Sigma-Aldrich), 5×10^5 trophic forms, and/or 5×10^5 mixed *P. murina* organisms at 37°C under 5.0% CO_2 for 72 h in BMDC culture medium. Supernatants were collected, centrifuged at $2,700 \times g$ for 1 min to remove organisms, and frozen for subsequent analysis of cytokine levels using IL-1β, IL-6, TNF-α, and IFN-γ enzyme-linked immunosorbent assay (ELISA) kits (eBioscience, San Diego CA). Trypan blue (Sigma-Aldrich) was used to evaluate the viability of BMDCs following stimulation with 10 μg/ml curdlan, 5×10^5 trophic forms, and/or 5×10^5 mixed *P. murina* organisms at 37°C under 5.0% CO_2 for 72 h in BMDC culture medium.

Statistical analysis. Data were analyzed utilizing the SigmaStat statistical software package (SPSS Inc., Chicago, IL). Student's *t* test with one-way or two-way analysis of variance (ANOVA) was used to determine differences between groups, with Student-Newman-Keuls or Holm-Sidak multiple-comparison *post hoc* tests. Kruskal-Wallis one-way ANOVA on ranks was used to analyze differences between groups when the data were nonparametric. Data were determined to be significantly different when the *P* value was ≤0.05.

RESULTS

***P. murina* trophic forms encyst by day 14 postinfection in neonatal mice.** Recent evidence indicates that cysts are the transmittable life cycle stage of *Pneumocystis* species (24). However, there is a paucity of data regarding how the immune system handles the trophic forms of the organisms. We previously published a report that alveolar macrophages from either adult or neonatal mice failed to translocate NF-κB in response to trophic forms (9). Therefore, we first wanted to know how the immune response differed when cysts were absent early in the infection and how quickly after infection trophic forms transitioned to cysts. To evaluate the differential immune response to the life cycle stages, we infected wild-type neonatal mice with either pure trophic forms or a physiologically normal mixture of *P. murina* trophic forms and cysts (Fig. S1 in the supplemental material). Neonatal mice infected with a normal mixture of *P. murina* organisms fail to mount adaptive immune responses until the age of 21 days (9). This presents an opportunity to observe the growth of the life cycle stages of *P. murina* in the absence of protective responses.
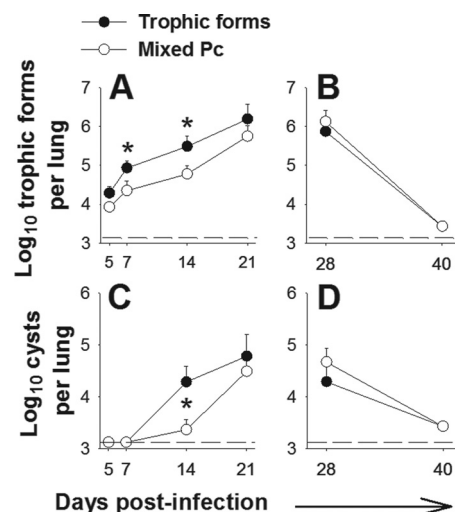

FIG 1 Cysts are undetectable during the first week postinfection in BALB/cJ neonates infected with *P. murina* trophic forms. Neonatal (24- to 72-h-old) mice were infected i.n. with 10^6 trophic forms or mixed *P. murina* organisms. Trophic (A and B) and cystic (C and D) burdens in the right lung lobes were determined by enumeration of organisms on Diff-Quik-stained slides under a microscope. Data are means ± standard deviations for 3 to 4 mice per group and are representative of 2 separate experiments. The limit of detection was $\log_{10}$ 3.12 nuclei per neonatal right lung lobe. Two-way ANOVA with a Holm-Sidak *post hoc* test was used to compare mean trophic form or cyst numbers between the groups. *, $P \le 0.05$.

Trophic forms were detected at day 5 postinfection in the lungs of BALB/cJ neonates infected with 1×10^6 trophic forms or 1×10^6 mixed *P. murina* organisms (Fig. 1A). The mixed *P. murina* inoculum consisted of 9.01×10^5 trophic forms and 9.90×10^4 cysts. Neonates infected with trophic forms had higher trophic burdens in the lungs at days 7 and 14 postinfection than mice infected with mixed *P. murina* organisms (Fig. 1A). However, the trophic lung burdens in the two groups were similar by day 21 postinfection (Fig. 1A and B). The cyst burden was below the limit of detection of $\log_{10}$ 3.12 organisms per lung during the first week postinfection in BALB/cJ neonates infected with either trophic forms or mixed *P. murina* organisms (Fig. 1C). Cysts were detected at day 14 postinfection in both groups. Neonates infected with trophic forms had higher cyst burdens in the lungs at day 14 postinfection than mice infected with mixed *P. murina* organisms, but there was no statistically significant difference in the cyst burden between the groups by day 21 postinfection (Fig. 1C). Neonates infected with trophic forms and those infected with mixed *P. murina* organisms displayed no differences in the clearance of either trophic forms or cysts (Fig. 1B and D).

Cysts drive the early recruitment of activated T cells into the alveolar spaces of neonatal mice. Based on previously published reports, we predicted that the absence of cysts in the inoculum of neonatal mice infected with trophic forms would yield a less robust response than infection with a normal mixture of trophic forms and cysts (22). Clearance of *Pneumocystis* organisms requires the generation of effective adaptive immune responses. We have shown previously that adaptive responses are not observed in immunocompetent neonatal mice until week 3 postinfection (9). To determine if the absence of cysts in the inoculum affects the neonatal adaptive immune response, T and B cells in the lungs of neonates infected with trophic forms were compared with those of
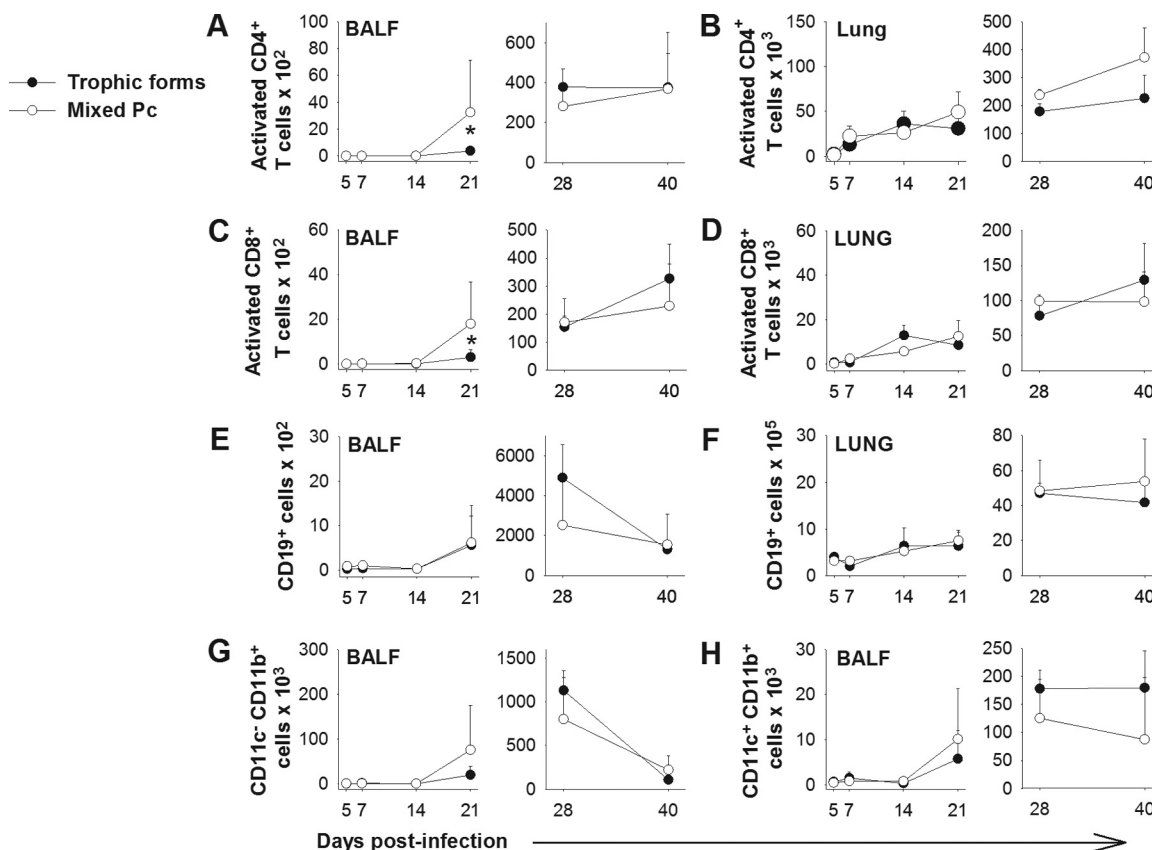
FIG 2 Cysts promote the recruitment of activated T cells in the BALF by day 21 postinfection in neonates. Neonatal (24- to 72-h-old) BALB/cJ mice were infected i.n. with 10^6 trophic forms or mixed *P. murina* organisms. (A though F) Flow cytometry was used to phenotype activated $CD44^{high}$ $CD62L^{low}$ $CD4^+$ T cells (A and B), activated $CD44^{high}$ $CD62L^{low}$ $CD8^+$ T cells (C and D), and $CD19^+$ B cells (E and F) in the BALF and lung digest. (G and H) Flow cytometry was used to phenotype $CD11c^-$ $CD11b^+$ (G) and $CD11c^+$ $CD11b^+$ (H) nonlymphocytes with high granularity and size from the BALF. Data are means ± standard deviations for 3 to 4 mice per group and are representative of 2 separate experiments. For comparison of mean total cell numbers between the groups at individual time points, *t* tests were used. *, $P \le 0.05$.

neonates infected with a normal mixture of *P. murina* organisms. The numbers of activated $CD44^{high}$ $CD62L^{low}$ $CD4^+$ and $CD8^+$ T cells in the alveolar spaces (represented by cells collected in the BALF) were significantly higher by week 3 postinfection in pups infected with organisms that included cysts in the inoculum than in pups infected with trophic forms only (Fig. 2A and C). No differences were observed in the numbers of T cells in the lung parenchyma (lung digest) (Fig. 2B and D). These data indicate that the intensity of the early T cell response to *P. murina* in the alveolar spaces is dependent on the presence of cysts in the inoculum. The numbers of $CD19^+$ B cells in the lungs did not differ between pups infected with mixed *P. murina* organisms and those infected with trophic forms (Fig. 2E). The numbers of activated T cells and $CD19^+$ B cells in the alveolar spaces and lung parenchyma were equivalent for the two groups at days 28 and 40 postinfection.

To determine if the absence of cysts in the inoculum affects the neonatal innate immune response, the expansion or recruitment of alveolar or nonresident innate immune cells in neonatal mice infected with trophic forms was compared with that in neonates infected with a normal mixture of *P. murina* organisms. The level of recruitment of $CD11c^-$ $CD11b^+$ nonresident innate immune cells to the alveolar spaces (BALF) by week 3 postinfection was higher in mice infected with mixed *P. murina* organisms than in

those infected with trophic forms alone, but these differences were not statistically significant (Fig. 2G). The numbers of $CD11c^+$ $CD11b^+$ innate immune cells increased by 3 weeks postinfection in the alveolar spaces of neonates infected with either trophic forms or mixed *P. murina* organisms (Fig. 2H). There were no differences in these responses between the groups at days 28 and 40 postinfection (Fig. 2G and H).

P. murina trophic forms encyst by day 7 postinfection in adult mice. Quantification of the fungal lung burden in neonatal mice demonstrates that the cysts were below the limit of detection during the first week after infection with either trophic forms or mixed *P. murina* organisms. To determine if similar kinetics would be observed in adults, we infected immunocompetent BALB/cJ adult mice with trophic forms or mixed *P. murina* organisms. Trophic forms were detected at day 5 postinfection in the lungs of adults infected with trophic forms or mixed *P. murina* organisms (Fig. 3A and C). Cysts were first detected at day 7 postinfection in the lungs of adults infected with trophic forms or mixed *P. murina* organisms (Fig. 3B and D). The trophic and cystic lung burdens were similar for the two groups at all time points and peaked at day 14 postinfection (Fig. 3A to D). The difference in the cyst burden at day 7 postinfection (Fig. 3B) was not consistent in a repeat of the experiment (Fig. 3D). The trophic and cystic lung burdens were below, or approaching, the limit of
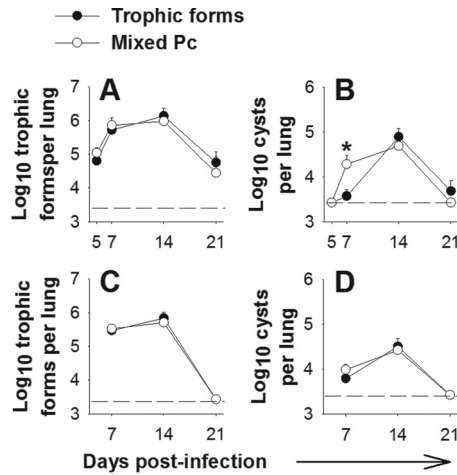
FIG 3 Cysts are undetectable before day 7 postinfection in BALB/cJ adults infected with *P. murina* trophic forms. Adult mice were infected i.t. with 5 × 10⁶ trophic forms or mixed *P. murina* organisms. Trophic (A and C) and cystic (B and D) lung burdens from two separate experiments were determined by enumeration of organisms on Diff-Quik-stained slides under a microscope. Data are means ± standard deviations for 5 mice per group. The limit of detection was log₁₀ 3.42 nuclei per adult right lung lobe. For comparison of mean fungal burdens between the two groups at individual time points, *t* tests were used. *, $P \leq 0.05$.

FIG 4 Infection with the cyst life cycle stage drives the recruitment of T and B cells into the lungs of adult mice. Adult BALB/cJ mice were infected i.t. with 5 × 10⁶ trophic forms or mixed *P. murina* organisms. Flow cytometry was used to phenotype activated CD4⁺ T cells (A), activated CD8⁺ T cells (B), and CD19⁺ B cells (C) in the BALF, lung digest, and TBLN. Activation of T cells was evaluated by CD44 and CD62L expression. Data are means ± standard deviations for 5 mice per group and are representative of 2 separate experiments. For comparison of mean total cell numbers between the groups at individual time points, *t* tests were used. *, $P \leq 0.05$; **, $P \leq 0.01$; ***, $P \leq 0.001$.

detection of log₁₀ 3.42 organisms per lung by day 21 postinfection, indicating that there were no differences in the clearance of *P. murina* organisms between the groups (Fig. 3A to D).

Cysts drive the early recruitment of T and B cells into the lungs of adult mice. To determine if cysts are required for the early recruitment of T and B cells into the lungs of immunocompetent adult mice, we infected adult BALB/cJ mice with either trophic forms or a normal mixture of *P. murina* organisms (Fig. 4). The robust early recruitment of activated CD44^high CD62L^low CD4⁺ and CD8⁺ T cells into the alveolar spaces (BALF) was dependent on the presence of cysts in the inoculum (Fig. 4A and B). Higher numbers of activated CD4⁺ and CD8⁺ T cells were also observed at day 5 postinfection in the lung parenchyma of mice infected with a mixture of trophic forms and cysts than in that of mice infected with trophic forms alone (Fig. 4A and B). Cysts in the inoculum also promoted the early recruitment of CD19⁺ B cells into the alveolar spaces and an early increase in the number of CD19⁺ B cells in the TBLN (Fig. 4C). T and B cell numbers in mice infected with trophic forms were similar to or greater than those in mice infected with mixed *P. murina* organisms as the mice approached clearance at week 3 postinfection.

Cysts promote the early infiltration of nonresident innate immune cells in adult mice. The level of recruitment of CD11c⁻ CD11b⁺ nonresident innate immune cells to the alveolar spaces (BALF) and lung parenchyma (lung digest) of adult BALB/cJ mice by day 14 postinfection was higher in mice infected with cysts in the inoculum than in those infected with trophic forms alone (Fig. 5A). The numbers of CD11c⁺ CD11b⁺ innate immune cells increased during the first week postinfection in the alveolar spaces and parenchyma of adults infected with mixed *P. murina* organisms (Fig. 5B). The numbers of lung-resident CD11c⁺ CD11b⁻ innate immune cells increased in the lung parenchyma of adults infected with mixed *P. murina* organisms at day 5 postinfection, but no statistically significant differences were observed in the
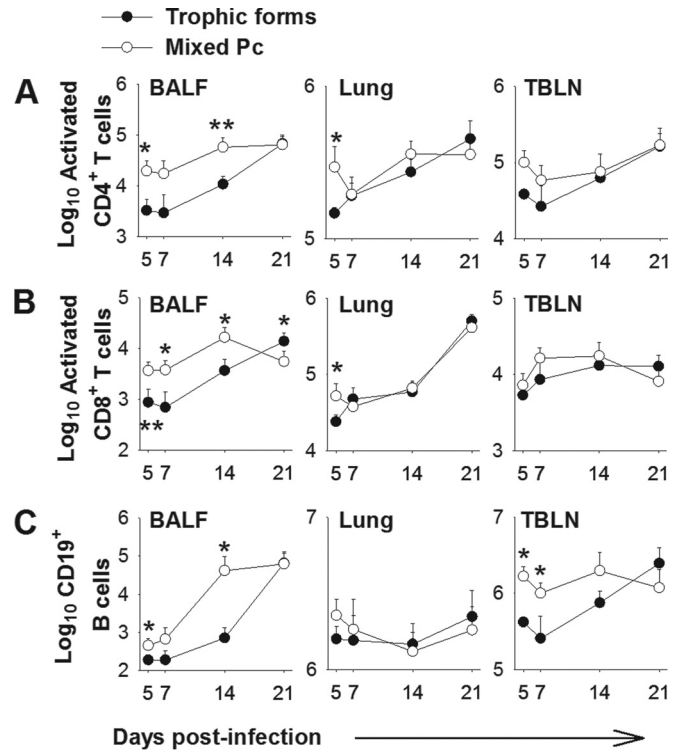
alveolar spaces between the two groups (Fig. 5C). Surface expression of the major histocompatibility complex (MHC) class II molecule I-A^d was higher on both CD11c⁺ CD11b⁻ and CD11c⁺ CD11b⁺ innate immune cells in the alveolar spaces of mice infected with mixed *P. murina* organisms than in those of mice infected with trophic forms alone (Fig. 5D and E). These data indicate that the presence of cysts in the initial inoculum shapes the phenotype of the early innate immune response in adult mice.

Cysts drive the early production of IFN-γ in the alveolar spaces of adult mice. T_h1-, T_h2-, and T_h17-type responses have all been associated with the clearance of *P. murina* organisms (25–27). To determine if cysts promoted the early development of T_h1-type responses in the lungs, we evaluated cytokine production following infection of BALB/cJ adult mice with either trophic forms or a normal mixture of *P. murina* organisms. The early production of IFN-γ in the BALF was higher in mice infected with cysts in the inoculum than in those infected with trophic forms alone (Fig. 6A). The level of IFN-γ production in the lungs of mice infected with trophic forms remained lower at all time points than that in mice infected with a mixture of *P. murina* organisms, despite the presence of cysts by day 7 postinfection (Fig. 6A). In addition, the proportion of CD4⁺ T cells producing intracellular IFN-γ at day 7 postinfection was higher in the lungs of mice in-
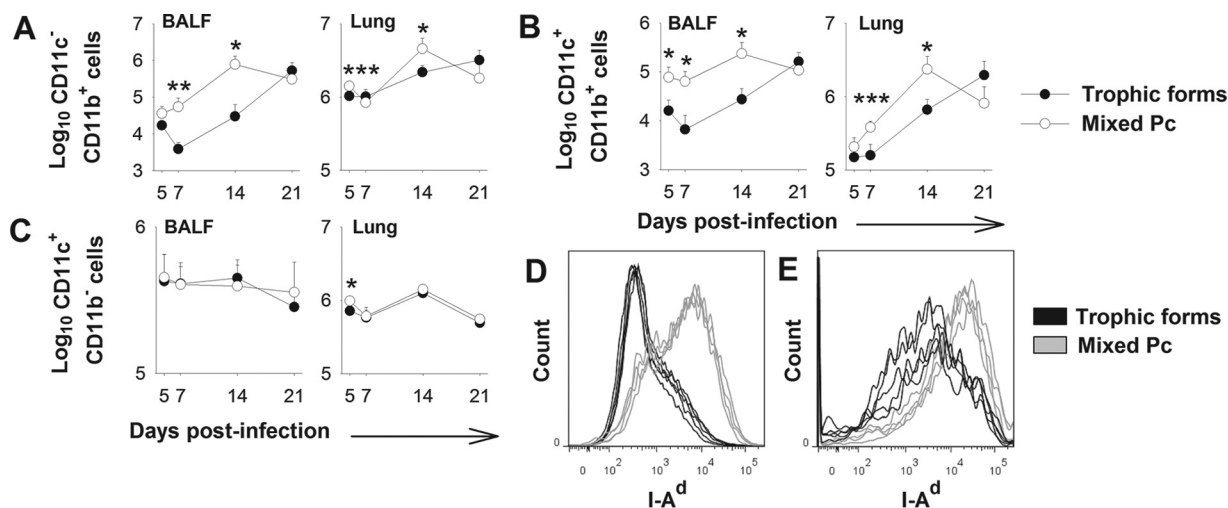
FIG 5 Cysts promote the early increase in CD11c$^+$ CD11b$^+$ innate immune cells and the infiltration of CD11c$^-$ CD11b$^+$ innate immune cells into the alveolar spaces and lung parenchyma of adult mice. BALB/cJ adult mice were infected i.t. with 5×10^6 trophic forms or mixed *P. murina* organisms. (A to C) Flow cytometry was used to phenotype CD11c$^-$ CD11b$^+$ (A), CD11c$^+$ CD11b$^+$ (B), and CD11c$^+$ CD11b$^-$ (C) nonlymphocytes with high granularity and size from the BALF and lung digest. (D and E) Flow cytometry was used to compare the expression of the MHC class II molecule I-A^d on CD11c$^+$ CD11b$^-$ (D) and CD11c$^+$ CD11b$^+$ (E) cells in the BALF. Data are means ± standard deviations for 5 mice per group and are representative of 2 separate experiments. For comparison of mean total cell numbers between the groups at individual time points, *t* tests were used. *, $P \leq 0.05$; **, $P \leq 0.01$; ***, $P \leq 0.001$.

fected with mixed *P. murina* organisms than in those of mice infected with trophic forms (Fig. 6B).

Trophic forms suppress β-glucan-induced proinflammatory cytokine production by dendritic cells. β-Glucan from the cell walls of *Pneumocystis* cysts has been shown previously to stimulate the production of IL-1β, IL-6, and TNF-α in dendritic cells and to induce IFN-γ production in cocultured T cells (21). To evaluate whether trophic forms are able to stimulate proinflammatory cytokines, we measured IL-1β, IL-6, and TNF-α production by bone marrow-derived dendritic cells (BMDCs) following stimulation with trophic forms, a normal mixture of *P. murina*

FIG 6 Cysts stimulate production of the proinflammatory T$_h$1-type cytokine IFN-γ in the lungs of adult BALB/cJ mice. Adult mice were infected i.t. with 5×10^6 trophic forms or mixed *P. murina* organisms. (A) IFN-γ cytokine production in the supernatant of the first bronchoalveolar lavage was quantified by ELISA. (B) Flow cytometry was used to evaluate intracellular IFN-γ expression in CD4$^+$ cells in the lung digest at day 7 postinfection. Data are means ± standard deviations for 5 mice per group and are representative of 2 separate experiments. For comparison of BALF IFN-γ levels between the groups at individual time points (A) and for comparison of the percentages of CD4$^+$ T cells expressing IFN-γ between the groups (B), *t* tests were used. **, $P \leq 0.01$.

organisms, and/or curdlan (Fig. 7). Curdlan is a high-molecular-weight β-1,3-glucan isolated from *Alcaligenes faecalis* and is homologous to the β-1,3-glucan that makes up the *P. murina* cyst wall (15). IL-1β and IL-6 production was stimulated by 5×10^5 mixed *P. murina* organisms and 10 μg/ml curdlan, but not by 5×10^5 trophic forms (Fig. 7A and B). These data demonstrate that cysts are required for the production of IL-1β and IL-6 by BMDCs. Stimulation of BMDCs with curdlan induced IL-1β, IL-6, and TNF-α production (Fig. 7A to C). Conversely, our data indicate that trophic forms suppress curdlan-induced IL-1β, IL-6, and TNF-α production by BMDCs in a dose-dependent manner (Fig. 7A to C). Interestingly, 10^6 trophic forms suppressed the IL-6 production induced by 5×10^5 mixed *P. murina* organisms (Fig. 7B) but were insufficient to induce suppression of IL-1β production (Fig. 7A). In contrast to IL-1β and IL-6 production, TNF-α production was stimulated by curdlan, but not by trophic forms or mixed *P. murina* organisms (Fig. 7C). Moreover, incubation of BMDCs with a high number of trophic forms or mixed *P. murina* organisms suppressed curdlan-induced production of TNF-α (Fig. 7C). This reduction in the level of cytokine production was not due to a toxic effect on the BMDCs (see Fig. S2 in the supplemental material).

The *P. murina* cell wall has been shown to contain more-complex branching patterns, including β-1,6-glucan, than those contained in curdlan. The *P. murina* cell wall also includes mannosylated proteins. To evaluate the ability of trophic forms to suppress responses to a fungal cell wall, we measured cytokine production following stimulation with trophic forms, zymosan, and/or depleted zymosan (see Fig. S3 in the supplemental material). Zymosan is a protein-carbohydrate preparation from the cell wall of *Saccharomyces cerevisiae*. Depleted zymosan is treated with hot alkali to prevent engagement of the Toll-like receptors (TLRs). Trophic forms suppressed the production of IL-1β, IL-6, and TNF-α induced by zymosan or depleted zymosan.

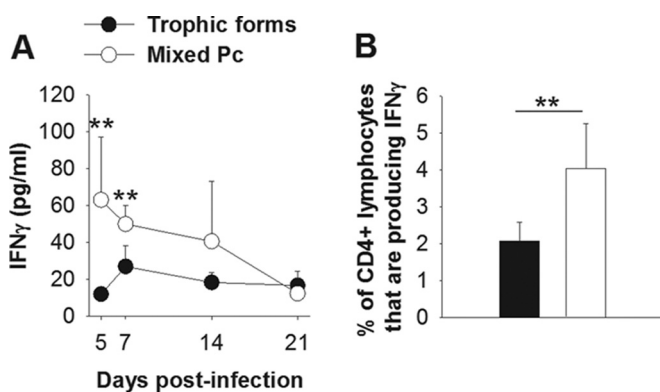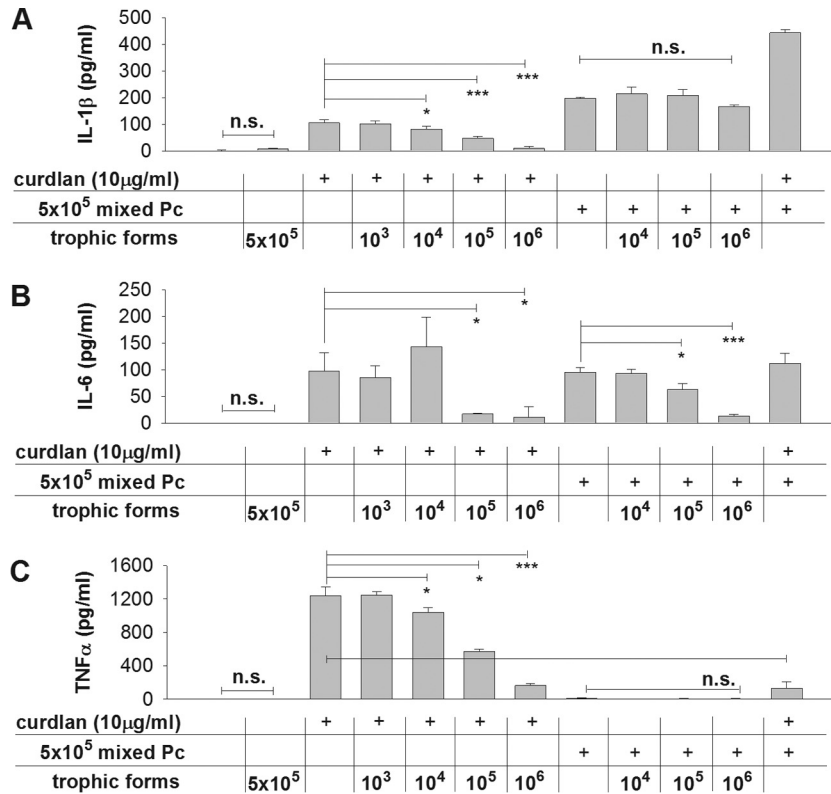To evaluate whether dendritic cells are able to present antigen

FIG 7 Cysts, but not trophic forms, stimulate production of the proinflammatory cytokines IL-1β and IL-6 by BMDCs *in vitro*. BMDCs from adult BALB/cJ mice were incubated with 5×10^5 trophic forms or 5×10^5 mixed *P. murina* organisms for 72 h. Curdlan was included as a positive control for cytokine production. IL-1β (A), IL-6 (B), and TNF-α (C) cytokine production was quantified by ELISA. Data are means ± standard deviations for 3 biological replicates per group and are representative of at least 2 separate experiments. One-way ANOVA with a Student-Newman-Keuls *post hoc* test was used to compare supernatant cytokine concentrations between the groups. *, $P \leq 0.05$; **, $P \leq 0.01$; ***, $P \leq 0.001$; n.s., not statistically significant.

and induce T_h1-type responses when loaded with trophic forms, we stimulated BMDCs cocultured with CD4+ T cells with either mixed *P. murina* organisms or trophic forms. BMDCs loaded with mixed *P. murina* organisms, but not with trophic forms, stimulated IFN-γ production in CD4+ T cells (Fig. 8). The addition of curdlan did not improve IFN-γ production in response to trophic forms (data not shown). These data demonstrate that cysts are
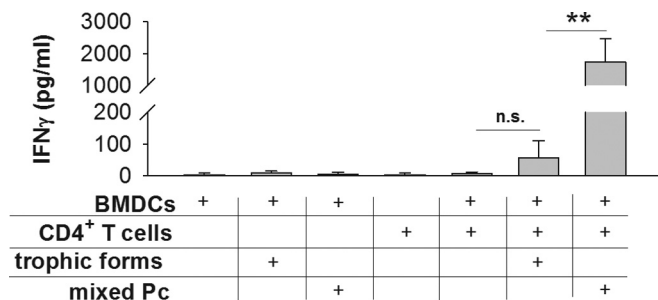

FIG 8 Cysts, but not trophic forms, stimulate production of the proinflammatory T_h1-type cytokine IFN-γ by CD4+ T cells *in vitro*. CD4+ T cells and BMDCs from adult BALB/cJ mice were incubated with trophic forms or mixed *P. murina* organisms for 72 h. IFN-γ cytokine production was quantified by ELISA. Data are means ± standard deviations for 3 biological replicates per group and are representative of 3 separate experiments. One-way ANOVA with a Student-Newman-Keuls *post hoc* test was used to compare supernatant IFN-γ concentrations between the groups. **, $P \leq 0.01$; n.s., not significant.

required for effective T_h1-type responses *in vitro* and are consistent with our findings *in vivo* that cysts drive the early T cell response to *P. murina*.

Trophic forms suppress TLR2- and TLR4-induced proinflammatory cytokine production by dendritic cells. In addition to C-type lectin receptors such as dectin-1, *Pneumocystis* species have been shown to stimulate cytokine production by antigen-presenting cells via TLR2 and TLR4 (28, 29). We measured IL-1β, IL-6, and TNF-α production by BMDCs following stimulation with TLR2-agonist LTA, TLR4-agonist LPS, and/or trophic forms (Fig. 9). Stimulation of BMDCs with LTA or LPS induced IL-1β, IL-6, and TNF-α production (Fig. 9A to F). The addition of 5×10^5 trophic forms suppressed this cytokine response to LTA and LPS.

The suppression of the response to curdlan is not mediated by mannose receptor. Carbohydrate PAMPs on the surfaces of fungi and other microorganisms may be recognized by C-type lectin receptors. Mannose receptor and dectin-1 have been implicated in the immune response to *Pneumocystis* species (30–35). To evaluate the role of mannose receptor and dectin-1 in the response to trophic forms and β-glucan, we stimulated BMDCs deficient in those C-type lectin receptors with trophic forms, mixed *P. murina* organisms, and/or curdlan (Fig. 10). Surprisingly, neither mannose receptor nor dectin-1 was required for IL-6 or TNF-α production in response to mixed *P. murina* organisms. IL-1β production in response to mixed *P. murina* organisms
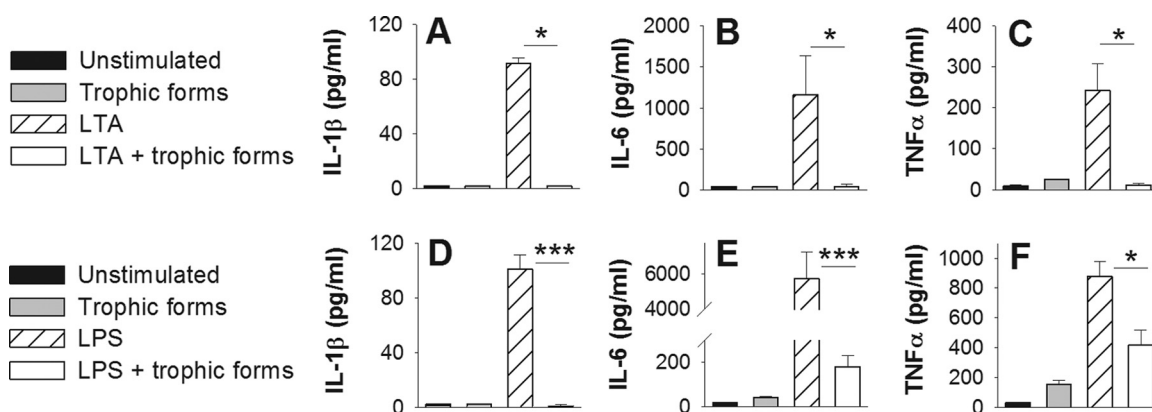
FIG 9 Trophic forms suppress LTA- and LPS-mediated cytokine production. BMDCs from adult BALB/cJ mice were incubated with 5×10^5 trophic forms, 10 μg/ml LTA (A to C), and/or 100 ng/ml LPS (D to F) for 72 h. IL-1β (A and D), IL-6 (B and E), and TNF-α (C and F) cytokine production was quantified by ELISA. Data are means ± standard deviations for 3 biological replicates per group and are representative of 3 separate experiments. One-way ANOVA with a Student-Newman-Keuls *post hoc* test was used to compare supernatant cytokine concentrations among the groups when the data were parametric (D and E) (***, $P \leq 0.001$). Kruskal-Wallis one-way ANOVA on ranks was used to compare differences among the groups when the data were nonparametric (A, B, C, and F) (*, $P \leq 0.05$).

was modestly dependent on dectin-1. As expected, mannose receptor was not responsible for the response to curdlan. Depletion of dectin-1 did not fully abolish the IL-6 and TNF-α responses to curdlan. It is possible that other receptors, such as complement receptor 3, may recognize this β-1,3-glucan or that the curdlan preparation contained additional PAMPs beyond β-1,3-glucan. Neither mannose receptor nor dectin-1 was exclusively required for the trophic-form-mediated suppression of IL-1β, IL-6, and TNF-α production. In the absence of mannose receptor or dectin-1, there was a modest increase in IL-6 production by BMDCs

treated with curdlan and trophic forms over that by wild-type BMDCs. Together, these data demonstrate that dectin-1 does not contribute significantly to the IL-1β, IL-6, or TNF-α response to mixed *P. murina* organisms but is involved in signaling β-glucan responses, though not exclusively. Furthermore, mannose receptor has only a minor role in the inhibitory effects of trophic forms on β-glucan stimulation of IL-6 production. These data suggest that other pattern recognition receptors are involved in signaling in both the proinflammatory and the suppressive functions of *P. murina* life forms.
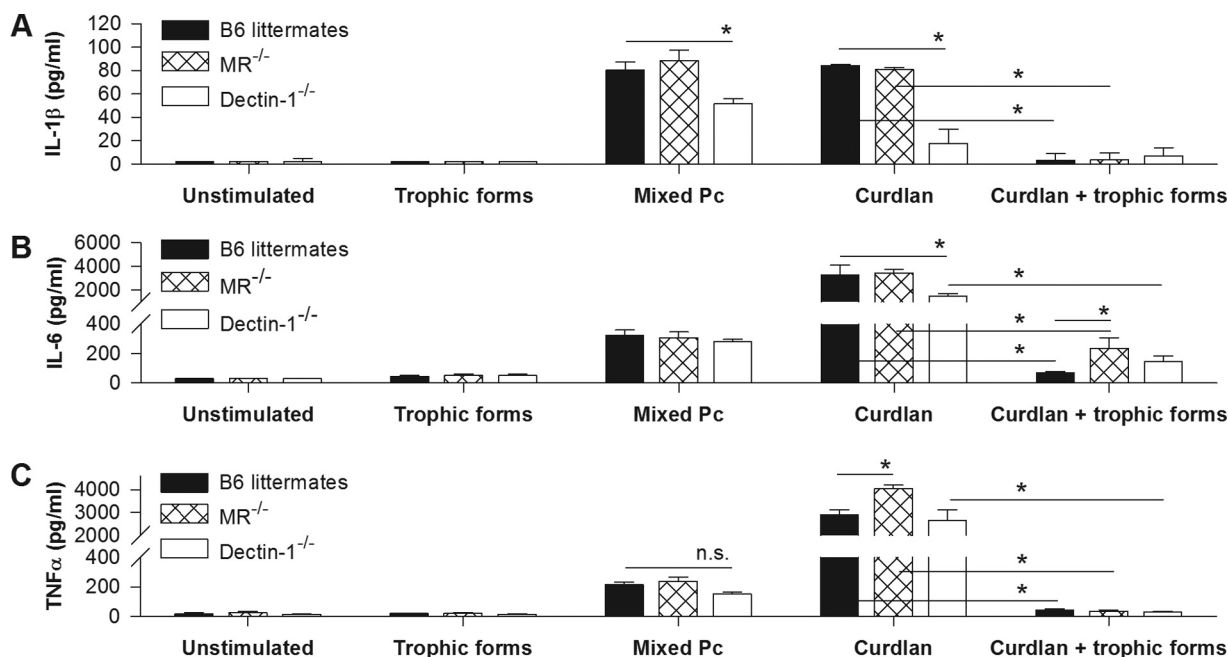

FIG 10 The response to trophic forms and cysts is not exclusively dependent on the C-type lectin receptors dectin-1 and mannose receptor. BMDCs from wild-type C57BL/6 littermate control, $MR^{-/-}$, and dectin-1 KO adult mice were incubated with 5×10^5 trophic forms or 5×10^5 mixed *P. murina* organisms for 72 h. Curdlan was included as a positive control for cytokine production. IL-1β (A), IL-6 (B), and TNF-α (C) cytokine production was quantified by ELISA. Data are means ± standard deviations for 3 biological replicates per group and are representative of 3 separate experiments. Kruskal-Wallis one-way ANOVA on ranks was used to compare differences among the groups when the data were nonparametric. *, $P \leq 0.05$.

DISCUSSION

Our data confirm that cysts drive immune responses to infection with *P. murina*. Cysts promote the early recruitment of activated CD4$^+$ and CD8$^+$ T cells into the lungs of neonatal and adult mice. Cysts also promote the early recruitment of nonresident innate immune cells and CD19$^+$ cells into the alveolar spaces of adult mice. Cysts in the inoculum stimulate the production of IFN-γ. Importantly, we found for the first time that trophic forms suppress β-glucan-, LTA-, and LPS-induced proinflammatory cytokine production by dendritic cells. Furthermore, dendritic cells cultured with trophic forms failed to stimulate the production of IFN-γ by CD4$^+$ T cells. Our data are consistent with the cyst life cycle stage driving proinflammatory responses that direct the early recruitment of innate and adaptive immune cells. However, the trophic life cycle forms dampen β-glucan- and TLR-induced inflammation. This is a novel finding and suggests that the two life forms of *Pneumocystis* balance the immune response to the organisms.

We have reported previously that there is a delay in the immune response to *P. murina* in neonatal mice relative to that in adults (9–12). Despite the delay, the immune response is sufficient to mediate the clearance of *P. murina* organisms. This delayed response represents a balance between clearance of a pathogen and avoidance of inflammatory damage during postpartum development. Here we report that cysts in the inoculum drive adaptive immune responses to *P. murina* in neonatal mice by day 21 postinfection. The fungal burdens in neonates infected with trophic forms or mixed *P. murina* organisms were similar by day 21 postinfection. These data suggest that the composition of the inoculum shapes the immune responses that will eventually develop.

Redundant T$_h$1-, T$_h$2-, and T$_h$17-type responses are associated with the clearance of *Pneumocystis* organisms (1, 3, 4, 25–27). Here we report that cysts are required in the inoculum to stimulate the production of intracellular IFN-γ by CD4$^+$ T cells in adult mice at day 7 postinfection. CD8$^+$ T cells are not required for the clearance of *Pneumocystis* organisms but contribute to the production of proinflammatory cytokines, including IFN-γ, that mediate effector responses (36). The concentration of extracellular IFN-γ in the alveolar spaces of adult mice infected with trophic forms did not change over the course of infection, despite eventual increases in the cyst burden and the numbers of activated CD4$^+$ and CD8$^+$ T cells. This may suggest that trophic forms suppress T$_h$1-type responses, which would be consistent with our *in vitro* data.

Mice infected with trophic forms developed detectable cysts by day 7 (in adults) or day 14 (in neonates) postinfection. We were unable to discern in our models whether trophic forms are capable of inducing protective immune responses or whether the response to trophic forms is merely delayed. The reduced ability of trophic forms to stimulate IFN-γ expression does not preclude the generation of protective responses, since there is redundancy in the types of T helper responses that can mediate the clearance of *Pneumocystis* organisms (25–27). It has been reported previously (22), and our preliminary data using an echinocandin to prevent the formation of cysts suggest, that infection with trophic forms is sufficient to generate protective CD4$^+$ T cell and antibody responses (data not shown).

Clearance of *Pneumocystis* organisms is also dependent on al-veolar macrophage responses (2). Our data demonstrate that cysts drive increases in the numbers of CD11c$^+$ CD11b$^+$ lung-resident innate immune cells. This population includes activated alveolar macrophages (9). We found that cysts promote MHC class II expression on the surfaces of immune cells in the alveolar spaces. Decreased antigen presentation in the absence of cysts may have contributed to the less-robust T cell response observed in mice infected with trophic forms. Additionally, cysts drive the early infiltration of CD11c$^-$ CD11b$^+$ innate immune cells into the lungs. This population consists of monocytes, small macrophages, and neutrophils. Neutrophils are not required for clearance, but their accumulation in the lungs correlates with disease severity in human *Pneumocystis* pneumonia patients (5, 37).

Infection with trophic forms in the absence of cysts leads to the establishment of an immunosuppressive environment in the lungs that persists for as long as 1 week following the formation of the cystic stage. If cysts are in the inoculum, the trophic form is unable to suppress inflammatory responses in the lungs as definitively. We predict that infection with pure cysts, in the absence of trophic forms, would lead to accelerated inflammatory responses compared to those induced by infection with a mixture of organisms. Unfortunately, there is no reliable method for isolating *P. murina* cysts in appreciable quantities.

Other groups report difficulties in stimulating IL-1β, IL-6, and TNF-α cytokine production by antigen-presenting cells using unopsonized mixed *P. murina* organisms (34). We found that a multiplicity of infection of 50 mixed *P. murina* organisms to 1 BMDC was sufficient to induce IL-1β and IL-6 production. We attribute the necessity of this relatively high multiplicity of infection to the presence of trophic forms in the mixture, since our data demonstrate that trophic forms suppressed the production of the β-glucan-induced proinflammatory cytokines IL-1β, IL-6, and TNF-α by BMDCs. A multiplicity of infection of 50 *P. murina* organisms per dendritic cell is composed of approximately 5 cysts capable of stimulating positive cytokine responses plus 45 trophic forms, which will act to suppress these responses. Preliminary gene expression data demonstrate that BMDCs stimulated with curdlan or mixed *P. murina* organisms, but not with trophic forms, express IL-1β, IL-6, and TNF-α mRNAs (data not shown). This suggests that the trophic forms suppress cytokine production rather than cytokine secretion.

Interestingly, mixed *P. murina* organisms also failed to induce TNF-α in BMDCs in our model. TNF-α production is associated with protection against *P. murina*, and has been reported in BMDCs following stimulation with β-glucan extracted from the cell wall of the cyst life cycle stage (21). We propose that trophic forms, which make up approximately 90% of the organisms in mixed *P. murina* infection, are sufficient to suppress the production of TNF-α by BMDCs, which would otherwise be induced by β-glucan on the surfaces of the cysts. In agreement with this contention, we found that trophic forms inhibited cytokine production by curdlan-stimulated BMDCs.

C-type lectin receptors are transmembrane proteins that bind carbohydrates (38). Activation triggers phagocytosis, as well as signaling cascades that culminate in the activation of antigen-presenting cells and the production of inflammatory cytokines. Dendritic cells have been shown to respond to *Pneumocystis* cyst wall β-glucans via dectin-1 (21). Dectin-1 is required for the generation of an effective response to *Pneumocystis* infection (35). Previous work has shown that mannose receptor binds glycoprotein

A on the surfaces of *Pneumocystis* cells, triggering phagocytosis, reactive oxygen species production, and NF-κB-mediated production of IL-8 (31–33). Here we demonstrate that neither dectin-1 nor mannose receptor was exclusively required for the production of IL-1β, IL-6, and TNF-α by BMDCs in response to *P. murina*. Our data suggest redundancy in the receptors that recognize cysts and trophic forms.

Conversely, some C-type lectin receptors may suppress proinflammatory responses. Engagement of the C-type lectin receptor mincle by the fungal skin pathogen *Fonsecaea monophora* has been shown to suppress proinflammatory responses induced by dectin-1-mediated signaling (39). Zhang et al. demonstrated that blockage or knockdown of mannose receptor on rat alveolar macrophages resulted in elevated TNF-α production in response to unopsonized mixed *Pneumocystis* organisms (34). Here we demonstrate that the deletion of mannose receptor on dendritic cells resulted in a modest decrease in the ability of trophic forms to suppress the production of IL-6 in response to β-glucan, indicating that suppression is mediated through mechanisms other than mannose receptor. We are currently examining whether mincle could mediate the suppressive activity of trophic forms, as was found for *F. monophora*.

Our data indicate that trophic forms suppress cytokine responses to the TLR2 agonist LTA and the TLR4 agonist LPS. In one paper, mice with mutant TLR4 were shown to have reduced IL-10, IL-12p40, and MIP-2 levels in the BALF of *Pneumocystis*-infected mice and enhanced levels of TNF and IL-6, with no difference in the clearance of the organisms (28). In addition, dectin-1 acts synergistically with TLR2 and TLR4 to promote cytokine production following stimulation with curdlan (40). Simultaneous inhibition of dectin-1-, TLR2-, and TLR4-mediated signals may permit the trophic forms to broadly dampen the proinflammatory response and protect the colonization of the immunocompetent host by *Pneumocystis* organisms. The suppression of zymosan- and depleted-zymosan-stimulated cytokine production provides further evidence that trophic forms broadly dampen the response to carbohydrate and protein agonists.

The inflammatory potential of the cysts in the face of a 10-fold excess of suppressive trophic forms should not be understated. The ability of trophic forms to suppress cytokine production is dose dependent, and our data suggest that slight changes in the ratio of trophic forms to cysts may shift the balance between suppression and stimulation. Increasing the trophic form-to-cyst ratio from 10:1 to 12:1 (by the addition of 10^5 trophic forms) is sufficient for the trophic forms to begin to reduce the IL-6 response to the mixed population. Our *in vivo* data indicate that the cyst burden remains low during the first week postinfection but that cysts in the inoculum drive the initial inflammation. The rapid establishment of an immunosuppressive trophic population may be critical for avoiding preemptive detection and clearance by immunocompetent hosts. Conversely, immunocompromised mice with severe pneumonia experience a final burst of trophic growth, in which the ratio of trophic forms to cysts reaches a level as high as 30:1 (unpublished observation). This population shift may prolong the life of the immunocompromised host by dampening inflammation and may extend the window of opportunity for the transmission of cysts to additional hosts.

The inoculation with trophic forms employed in this study does not mimic the natural route of infection, since cysts are the transmittable life cycle stage of *Pneumocystis* species (24). In accordance with our goal, our approach allows conclusions to be formed about the differential immune responses to the life cycle stages of *Pneumocystis* species. Recently, it was reported that treatment of immune-reconstituted mice with the β-1,3-D-glucan synthase inhibitor anidulafungin results in depletion of cysts, with the remaining trophic burden stimulating a much-reduced inflammatory response (22). Anidulafungin belongs to a drug class known as the echinocandins, which have been used in combination with other antifungals in the treatment of *Pneumocystis* pneumonia in human patients (41). Linke et al. propose that depletion of cysts would reduce inflammation-induced lung damage in patients (22). Our data corroborate this suggestion and highlight the need for greater understanding of the response to the trophic stage. We propose that depletion of the immunostimulatory cysts in the presence of the immunosuppressive trophic forms may hamper the ability of immunocompromised patients or infants to control the infection. However, the net outcome may be positive, since lung damage during *Pneumocystis* pneumonia is predominately due to the inflammatory immune response.

In summary, our data indicate that cysts are the primary form of *Pneumocystis* responsible for provoking adult and neonatal immune responses to infection with *P. murina*. These responses include infiltration of nonresident innate immune cells and the recruitment of CD19$^+$ B cells and activated CD4$^+$ and CD8$^+$ T cells. Cysts are required to stimulate the production of IFN-γ by CD4$^+$ T cells *in vitro* and in the alveolar spaces of immunocompetent adult mice. We found that trophic forms suppress β-glucan-induced proinflammatory cytokine production by dendritic cells. We propose that the suppression of immune responses by the trophic forms promotes the colonization of immunocompetent hosts by *Pneumocystis* and may be beneficial to immunocompromised hosts by dampening the inflammatory responses that contribute to lung pathology during PcP. This differential immune response to *Pneumocystis* trophic forms and cysts is most certainly a leading contributor to the success of the organisms as human pathogens.

ACKNOWLEDGMENT

FUNDING INFORMATION

REFERENCES

1. **Harmsen AG, Stankiewicz M.** 1990. Requirement for CD4$^+$ cells in resistance to *Pneumocystis carinii* pneumonia in mice. J Exp Med **172:**937–945. http://dx.doi.org/10.1084/jem.172.3.937.

2. **Limper AH, Hoyte JS, Standing JE.** 1997. The role of alveolar macrophages in *Pneumocystis carinii* degradation and clearance from the lung. J Clin Invest **99:**2110–2117. http://dx.doi.org/10.1172/JCI119384.

3. **Lund FE, Schuer K, Hollifield M, Randall TD, Garvy BA.** 2003. Clearance of *Pneumocystis carinii* in mice is dependent on B cells but not on *P. carinii*-specific antibody. J Immunol **171:**1423–1430. http://dx.doi.org/10.4049/jimmunol.171.3.1423.

4. **Marcotte H, Levesque D, Delanay K, Bourgeault A, de la Durantaye R, Brochu S, Lavoie MC.** 1996. *Pneumocystis carinii* infection in transgenic

B cell-deficient mice. J Infect Dis **173**:1034–1037. http://dx.doi.org/10.1093/infdis/173.4.1034.

5. Limper AH, Offord KP, Smith TF, Martin WJ, II. 1989. *Pneumocystis carinii* pneumonia. Differences in lung parasite number and inflammation in patients with and without AIDS. Am Rev Respir Dis **140**:1204–1209.

6. Miller RF, Allen E, Copas A, Singer M, Edwards SG. 2006. Improved survival for HIV infected patients with severe *Pneumocystis jirovecii* pneumonia is independent of highly active antiretroviral therapy. Thorax **61**:716–721. http://dx.doi.org/10.1136/thx.2005.055905.

7. Gajdusek DC. 1957. *Pneumocystis carinii*; etiologic agent of interstitial plasma cell pneumonia of premature and young infants. Pediatrics **19**:543–565.

8. Peglow SL, Smulian AG, Linke MJ, Pogue CL, Nurre S, Crisler J, Phair J, Gold JW, Armstrong D, Walzer PD. 1990. Serologic responses to *Pneumocystis carinii* antigens in health and disease. J Infect Dis **161**:296–306. http://dx.doi.org/10.1093/infdis/161.2.296.

9. Kurkjian C, Hollifield M, Lines JL, Rogosky A, Empey KM, Qureshi M, Brown SA, Garvy BA. 2012. Alveolar macrophages in neonatal mice are inherently unresponsive to *Pneumocystis murina* infection. Infect Immun **80**:2835–2846. http://dx.doi.org/10.1128/IAI.05707-11.

10. Garvy BA, Harmsen AG. 1996. Susceptibility to *Pneumocystis carinii* infection: host responses of neonatal mice from immune or naïve mothers and of immune or naïve adults. Infect Immun **64**:3987–3992.

11. Garvy BA, Qureshi MH. 2000. Delayed inflammatory response to *Pneumocystis carinii* infection in neonatal mice is due to an inadequate lung environment. J Immunol **165**:6480–6486. http://dx.doi.org/10.4049/jimmunol.165.11.6480.

12. Qureshi MH, Garvy BA. 2001. Neonatal T cells in an adult lung environment are competent to resolve *Pneumocystis carinii* pneumonia. J Immunol **166**:5704–5711. http://dx.doi.org/10.4049/jimmunol.166.9.5704.

13. Cushion MT, Ruffolo JJ, Walzer PD. 1988. Analysis of the developmental stages of *Pneumocystis carinii, in vitro*. Lab Invest **58**:324–331.

14. Cushion MT, Collins MS, Linke MJ. 2009. Biofilm formation by *Pneumocystis* spp. Eukaryot Cell **8**:197–206. http://dx.doi.org/10.1128/EC.00202-08.

15. Walker AN, Garner RE, Horst MN. 1990. Immunocytochemical detection of chitin in *Pneumocystis carinii*. Infect Immun **58**:412–415.

16. Kottom TJ, Hebrink DM, Jenson PE, Gudmundsson G, Limper AH. 2015. Evidence for proinflammatory β-1,6 glucans in the *Pneumocystis carinii* cell wall. Infect Immun **83**:2816–2826. http://dx.doi.org/10.1128/IAI.00196-15.

17. Gigliotti F, Stokes DC, Cheatham AB, Davis DS, Hughes WT. 1986. Development of murine monoclonal antibodies to *Pneumocystis carinii*. J Infect Dis **154**:315–322. http://dx.doi.org/10.1093/infdis/154.2.315.

18. Gigliotti F, Ballou LR, Hughes WT, Mosley BD. 1988. Purification and initial characterization of a ferret *Pneumocystis carinii* surface antigen. J Infect Dis **158**:848–854. http://dx.doi.org/10.1093/infdis/158.4.848.

19. De Stefano JA, Myers JD, Du Pont D, Foy JM, Theus SA, Walzer PD. 1998. Cell wall antigens of *Pneumocystis carinii* trophozoites and cysts: purification and carbohydrate analysis of these glycoproteins. J Eukaryot Microbiol **45**:334–343. http://dx.doi.org/10.1111/j.1550-7408.1998.tb04545.x.

20. Ma L, Chen Z, Huang DW, Kutty G, Ishihara M, Wang H, Abouelleil A, Bishop L, Davey E, Deng R, Deng X, Fan L, Fantoni G, Fitzgerald M, Gogineni E, Goldberg JM, Handley G, Hu X, Huber C, Jiao X, Jones K, Levin JZ, Liu Y, Macdonald P, Melnikov A, Raley C, Sassi M, Sherman BT, Song X, Sykes S, Tran B, Walsh L, Xia Y, Yang J, Young S, Zeng Q, Zheng X, Stephens R, Nusbaum C, Birren BW, Azadi P, Lempicki RA, Cuomo CA, Kovacs JA. 2016. Genome analysis of three *Pneumocystis* species reveals adaptation mechanisms to life exclusively in mammalian hosts. Nat Commun **7**:10740. http://dx.doi.org/10.1038/ncomms10740.

21. Carmona EM, Vassallo R, Vuk-Pavlovic Z, Standing JE, Kottom TJ, Limper AH. 2006. *Pneumocystis* cell wall beta-glucans induce dendritic cell costimulatory molecule expression and inflammatory activation through a Fas-Fas ligand mechanism. J Immunol **177**:459–467. http://dx.doi.org/10.4049/jimmunol.177.1.459.

22. Linke MJ, Ashbaugh A, Collins MS, Lynch K, Cushion MT. 2013. Characterization of a distinct host response profile to *Pneumocystis murina* asci during clearance of *Pneumocystis* pneumonia. Infect Immun **81**:984–995. http://dx.doi.org/10.1128/IAI.01181-12.

23. Harding CV, Canaday D, Ramachandra L. 2010. Choosing and preparing antigen-presenting cells. Curr Protoc Immunol Chapter 16:Unit 16.1. http://dx.doi.org/10.1002/0471142735.im1601s88.

24. Cushion MT, Linke MJ, Ashbaugh A, Sesterhenn T, Collins MS, Lynch K, Brubaker R, Walzer PD. 2010. Echinocandin treatment of *Pneumocystis* pneumonia in rodent models depletes cysts leaving trophic burdens that cannot transmit the infection. PLoS One **5**:e8524. http://dx.doi.org/10.1371/journal.pone.0008524.

25. Garvy BA, Wiley JA, Gigliotti F, Harmsen AG. 1997. Protection against *Pneumocystis carinii* pneumonia by antibodies generated from either T helper 1 or T helper 2 responses. Infect Immun **65**:5052–5056.

26. Rudner XL, Happel KI, Young EA, Shellito JE. 2007. Interleukin-23 (IL-23)–IL-17 cytokine axis in murine *Pneumocystis carinii* infection. Infect Immun **75**:3055–3061. http://dx.doi.org/10.1128/IAI.01329-06.

27. Myers RC, Dunaway CW, Nelson MP, Trevor JL, Morris A, Steele C. 2013. STAT4-dependent and -independent Th2 responses correlate with protective immunity against lung infection with *Pneumocystis murina*. J Immunol **190**:6287–6294. http://dx.doi.org/10.4049/jimmunol.1300431.

28. Ding K, Shibui A, Wang Y, Takamoto M, Matsuguchi T, Sugane K. 2005. Impaired recognition by Toll-like receptor 4 is responsible for exacerbated murine *Pneumocystis* pneumonia. Microbes Infect **7**:195–203. http://dx.doi.org/10.1016/j.micinf.2004.10.010.

29. Zhang C, Wang SH, Lasbury ME, Tschang D, Liao CP, Durant PJ, Lee CH. 2006. Toll-like receptor 2 mediates alveolar macrophage response to *Pneumocystis murina*. Infect Immun **74**:1857–1864. http://dx.doi.org/10.1128/IAI.74.3.1857-1864.2006.

30. Sancho D, Reis e Sousa C. 2012. Signaling by myeloid C-type lectin receptors in immunity and homeostasis. Annu Rev Immunol **30**:491–529. http://dx.doi.org/10.1146/annurev-immunol-031210-101352.

31. O'Riordan DM, Standing JE, Limper AH. 1995. *Pneumocystis carinii* glycoprotein A binds macrophage mannose receptors. Infect Immun **63**:779–784.

32. Ezekowitz RA, Williams DJ, Koziel H, Armstrong MY, Warner A, Richards FF, Rose RM. 1991. Uptake of *Pneumocystis carinii* mediated by the macrophage mannose receptor. Nature **351**:155–158. http://dx.doi.org/10.1038/351155a0.

33. Zhang J, Zhu J, Imrich A, Cushion M, Kinane TB, Koziel H. 2004. *Pneumocystis* activates human alveolar macrophage NF-κB signaling through mannose receptors. Infect Immun **72**:3147–3160. http://dx.doi.org/10.1128/IAI.72.6.3147-3160.2004.

34. Zhang J, Tachado SD, Patel N, Zhu J, Imrich A, Manfruelli P, Cushion M, Kinane TB, Koziel H. 2005. Negative regulatory role of mannose receptors on human alveolar macrophage proinflammatory cytokine release in vitro. J Leukoc Biol **78**:665–674. http://dx.doi.org/10.1189/jlb.1204699.

35. Saijo S, Fujikado N, Furuta T, Chung SH, Kotaki H, Seki K, Sudo K, Akira S, Adachi Y, Ohno N, Kinjo T, Nakamura K, Kawakami K, Iwakura Y. 2007. Dectin-1 is required for host defense against *Pneumocystis carinii* but not against *Candida albicans*. Nat Immunol **8**:39–46. http://dx.doi.org/10.1038/ni1425.

36. Kolls JK, Habetz S, Shean MK, Vazquez C, Brown JA, Lei D, Schwarzenberger P, Ye P, Nelson S, Summer WR, Shellito JE. 1999. IFN-γ and CD8$^+$ T cells restore host defenses against *Pneumocystis carinii* in mice depleted of CD4$^+$ T cells. J Immunol **162**:2890–2894.

37. Azoulay E, Parrot A, Flahault A, Cesari D, Lecomte I, Roux P, Saidi F, Fartoukh M, Bernaudin JF, Cadranel J, Mayaud C. 1999. AIDS-related *Pneumocystis carinii* pneumonia in the era of adjunctive steroids: implication of BAL neutrophilia. Am J Respir Crit Care Med **160**:493–499. http://dx.doi.org/10.1164/ajrccm.160.2.9901019.

38. Kawai T, Akira S. 2011. Toll-like receptors and their crosstalk with other innate receptors in infection and immunity. Immunity **34**:637–650. http://dx.doi.org/10.1016/j.immuni.2011.05.006.

39. Wevers BA, Kaptein TM, Zijlstra-Willems EM, Theelen B, Boekhout T, Geijtenbeek TB, Gringhuis SI. 2014. Fungal engagement of the C-type lectin mincle suppresses dectin-1-induced antifungal immunity. Cell Host Microbe **15**:494–505. http://dx.doi.org/10.1016/j.chom.2014.03.008.

40. Ferwerda G, Meyer-Wentrup F, Kullberg BJ, Netea MG, Adema GJ. 2008. Dectin-1 synergizes with TLR2 and TLR4 for cytokine production in human primary monocytes and macrophages. Cell Microbiol **10**:2058–2066. http://dx.doi.org/10.1111/j.1462-5822.2008.01188.x.

41. Armstrong-James D, Stebbing J, John L, Murungi A, Bower M, Gazzard B, Nelson M. 2011. A trial of caspofungin salvage treatment in PCP pneumonia. Thorax **66**:537–538. http://dx.doi.org/10.1136/thx.2010.135350.